

Pei-Chi Yang^{1,2}, Laura L. Perissinotti³, Yibo Wang³, Kevin R. DeMarco^{1,2}, Mao-Tsuen Jeng^{1,2}, Igor Vorobyov^{1,2}, Vladimir Yarov-Yarovoy¹, Sergei Y. Noskov³, and Colleen E. Clancy^{1,2}

¹ Department of Physiology and Membrane Biology, School of Medicine, University of California, Davis; ² Department of Pharmacology, School of Medicine, University of California, Davis;

³ Centre for Molecular Simulation, Department of Biological Sciences, University of Calgary

1. INTRODUCTION

Heart rhythm disturbances, such as long QT syndrome (LQTS), have been linked to mutations in cardiac ions channels, as well as unintended drug interactions with these channels [1-3]. Female sex has been shown to be an independent risk factor for both inherited and acquired LQTS and associated Torsades de Pointes (TdP) arrhythmias [1,6]. Sympathetic discharge, resulting e.g. from a sudden arousal induced by loud noise or emotional stress, is a major factor in triggering TdP in female LQTS patients [1]. Both experimental and clinical studies have demonstrated that this phenomenon is likely related to differential levels of sex hormones (estradiol, progesterone and testosterone) playing opposite roles in pro-arrhythmia proclivities, exacerbating or mitigating effects of ion channel mutations or drug-induced blockade. During the menstrual follicular phase (prior to ovulation), estrogen level is the highest, QT interval is longer and susceptibility to arrhythmias is increased. In the luteal phase (following ovulation) progesterone is increased and arrhythmic events associated with acquired and inherited LQTS are reduced. The differences in arrhythmia vulnerability during stages of the menstrual cycle likely reflect the effects that sex steroid hormones have on cardiac ion channels [1,6].

Menstrual cycle	17 β -estradiol (E2)	Progesterone (Pg)
Early follicular stage	0.1 nM	2.5 nM
Late follicular stage	1.0 nM	2.5 nM
Luteal stage	0.7 nM	40.6 nM

Estradiol (E2) has been shown to acutely inhibit a repolarizing rapidly activating delayed rectifier K⁺ current I_{Kr} , associated with a voltage gated channel K_v11.1 encoded by the human *Ether-à-go-go-Related Gene* (hERG), resulting in increased ventricular action potential duration and longer QT interval [1,9]. Progesterone and male sex hormone testosterone have opposite effects due to enhancing the slow delayed rectifier K⁺ current (I_{Ks}) through a NO-dependent signaling pathway and inhibiting (for the latter) the inward Ca²⁺ current (I_{Ca-L}) [1]. We developed multiscale mathematical models of acquired and inherited LQTS in human male and female ventricular myocytes and cardiac tissues by combining effects of a hormone, sympathetic stimulation and a hERG channel blocker, dofetilide, or hERG mutations. See reference [1] for more details.

2. METHODS

Functional models of cardiac cells and tissues:

1. We modified the channel conductances in the O'Hara-Rudy human model [4] based on recent experimental data of sex-differences in ion channel expression to develop "female" and "male" models, using experimentally observed reduction in expression of connexin 43 (Cx43) and repolarization currents including I_{Kr} , I_{Ks} , I_{K1} , and I_{to} compared to males [5]. I_{Kr} is shown below as an example.

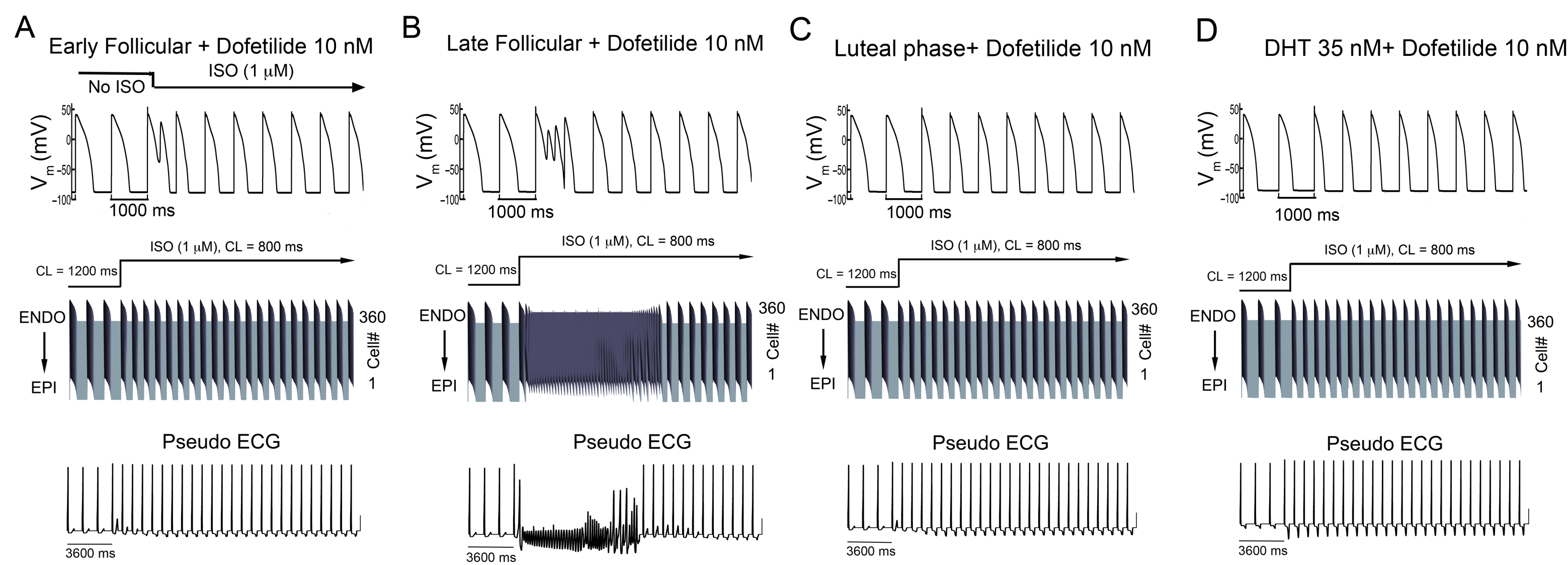
Channels in the model	Gene	Epi		Endo	
		Male	Female	Male	Female
I_{Kr}	hERG (K _v 11.1)	179.5 \pm 6.4 ↑	144.2 \pm 41.1 ↓	164.8 \pm 54.9 ↑	130.5 \pm 65 ↓
Ratio (Ratios are relative to the male endo cell)		1.09 \pm 0.039	0.875 \pm 0.25	1 \pm 0.33	0.79 \pm 0.39

- We incorporated effects of sex steroid hormones (acute effects) in the models, and PKA targets on I_{Na} , I_{CaL} , I_{Ks} , I_{NaK} , I_{Kb} and Ca²⁺ fluxes (J_{in} and J_{up}) and buffers (Troponin) [7].
- Experiments suggest that the G604S hERG pore loop mutation alters the current amplitude and the gating of the hERG channel. We simulated the mutant I_{Kr} (heterozygous channel = (WT + G604S)/2) by modifying the conductance of WT current and also the kinetics of WT channel from O'Hara-Rudy human model [4] based on the experimental data [3].
- Our I_{Kr} Markov model was incorporated into the O'Hara-Rudy human ventricular action potential model to simulate the effects of dofetilide on I_{Kr} [2].
- We simulated a transmural fiber composed of 360 ventricular cells ($\Delta x = \Delta y = 100 \mu m$) connected by resistances to simulate gap junctions. The fiber contains an endocardial region (cells 1 to 160) and epicardial region (cells 161 to 360), with a linear decrease in action potential duration (APD) as indicated by experimental data [8].
- We tested the vulnerability to arrhythmia induced by sympathetic nervous system (SNS) stimulation in models of LQTS by simulating a heterogeneous cardiac male and female 2D tissues (5.4 cm \times 6.6 cm) containing an endocardial region and an epicardial region based on recordings from human tissue [8].

Structural atomistic modeling and simulations:

- The SWISS-MODEL homology modeling program was used for the development of the hERG model from the Eag1 channel cryo-EM structure (PDB ID 5K7L). Developed closed-state hERG model was used to study interactions between E2 and extracellular pore-loop residues in both WT and G604S mutant.
- To study the potential interactions between the channel and E2 and/or hERG blocker dofetilide, we initially used a previously developed and experimentally validated model of the hERG pore in the open state [10] based on the K_v1.2 X-ray crystal structure (PDB ID 2A79).
- Recent hERG structure (PDB ID 5VA1) was used for molecular docking of d-sotalol and E2. Pore and voltage sensing domains (PD and VSD) comprising residues 405-668 were used. The missing loop regions were rebuilt via local iterative refinement with ROSETTA-Membrane.
- Molecular docking of dofetilide and/or E2 to hERG was performed using the Glide-XP and Induced Fit Docking modules of the Maestro suite by Schrödinger. Clustering analysis was used to evaluate the docking poses. The top-scoring poses were used for molecular dynamics (MD) simulations.
- ROSETTA-Ligand was used for d-sotalol and E2 docking simulations. 50,000 structures were generated in each run with top 10% selected by total score, out of which 50 with lowest interfacial score were chosen.
- CHARMM-GUI was used to prepare hERG + Dipalmitoylphosphatidylcholine (DPPC) lipid bilayer complexes solvated in 150 mM KCl aqueous solution using CHARMM36 force field, TIP3P water model and recently developed neutral dofetilide parameters [11]. MD simulations were run with NAMD using 10 ns equilibration and 50-100 ns production in the NPT ensemble at 315 K and 1 atm. The ensembles of MD frames were used for the calculation of binding enthalpies based on continuum solvent model [12].

3. Sex-based differences in human cardiac electrophysiology predicted in the setting of acquired Long-QT syndrome induced by dofetilide

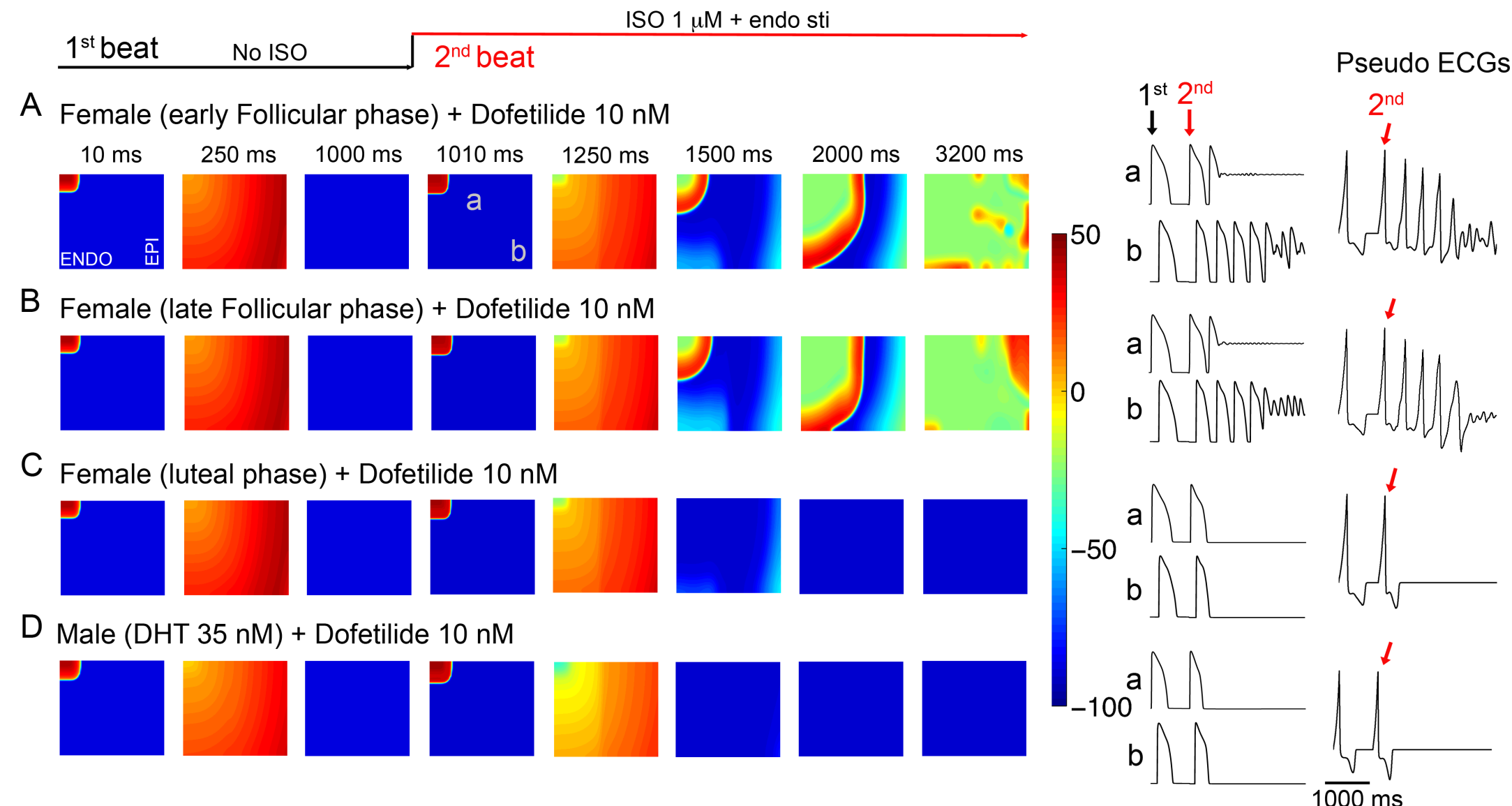


Upper panels: Single-cell action potential simulations predict that the female cells in the presence of a hERG blocker dofetilide exhibit arrhythmogenic rhythms upon sympathetic nervous system (SNS) stimulation during the late follicular phase (panel B).

Middle panels: 1D cable simulations show that an early after-depolarization (EAD) initiated in the endocardial region in the late follicular case (panel B) generates a sufficient source current to drive full action potential initiation in the downstream excitable (repolarized) epicardial region.

Lower panels: Pseudo ECG traces demonstrate abnormal rhythm only in the late follicular phase (panel B).

4. Female sex is predicted to increase susceptibility to reentrant arrhythmia following acute sympathetic nervous system (SNS) stimulations in the setting of acquired Long-QT syndrome induced by dofetilide

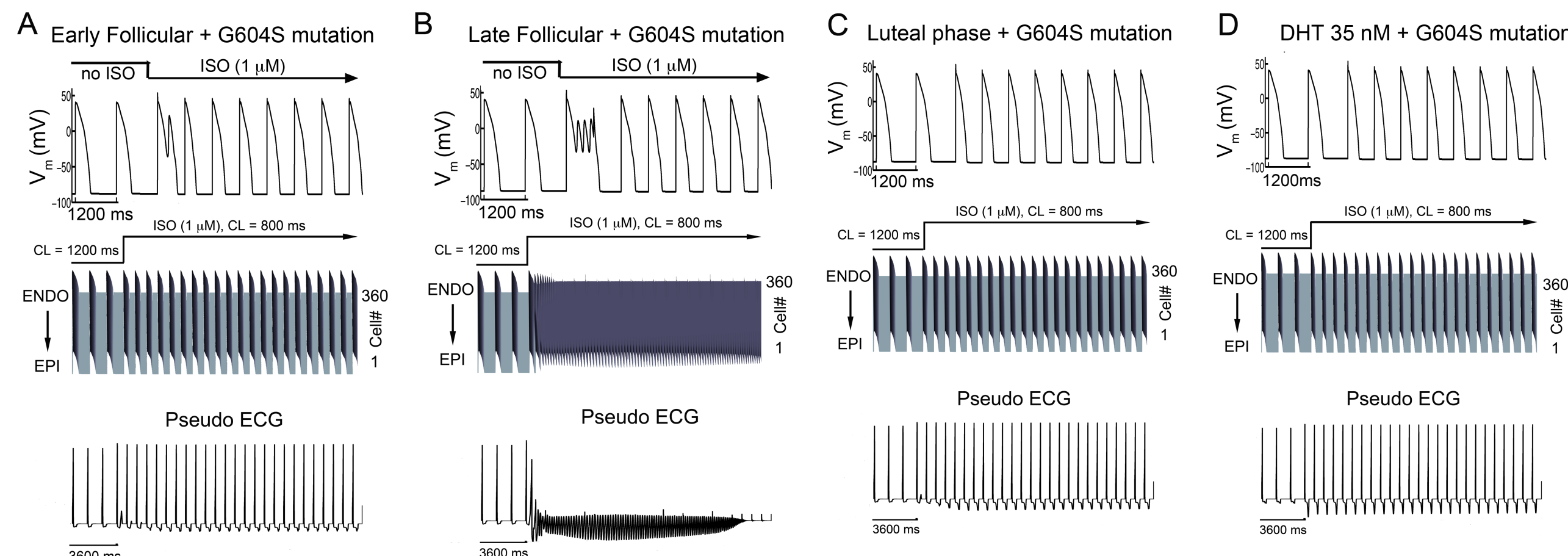


Predicted reentrant wave following SNS stimulations on female heterogeneous tissue (5.4 cm \times 6.6 cm containing an endocardial region in columns 1-160 and an epicardial region in columns 161-360), and anisotropic conduction in the presence of female hormones during the (A) early follicular, (B) late follicular, (C) luteal phases of the menstrual cycle, (D) in male tissue with 35nM testosterone. No arrhythmia was predicted in the luteal phase or male tissue.

The time course of single cell action potentials from two points in space (labeled as "a" and "b") in the simulated 2D tissue and the computed electrograms are shown in the right columns. Site "a" undergoes 2 consecutive stimuli (indicated as "1st" and "2nd") at 10 ms and 1010 ms.

Sympathetic activation occurs concurrently with the second stimulus. The tissue near site "a" then re-excites site "b", which continues in a feedback loop (observed as an oscillation on the computed electrogram), during which site "a" maintains depolarization and serves as a persistent current source.

5. Simulated arousal via sympathetic stimulation in the setting of the G604S mutation causing inherited LQTS type 2

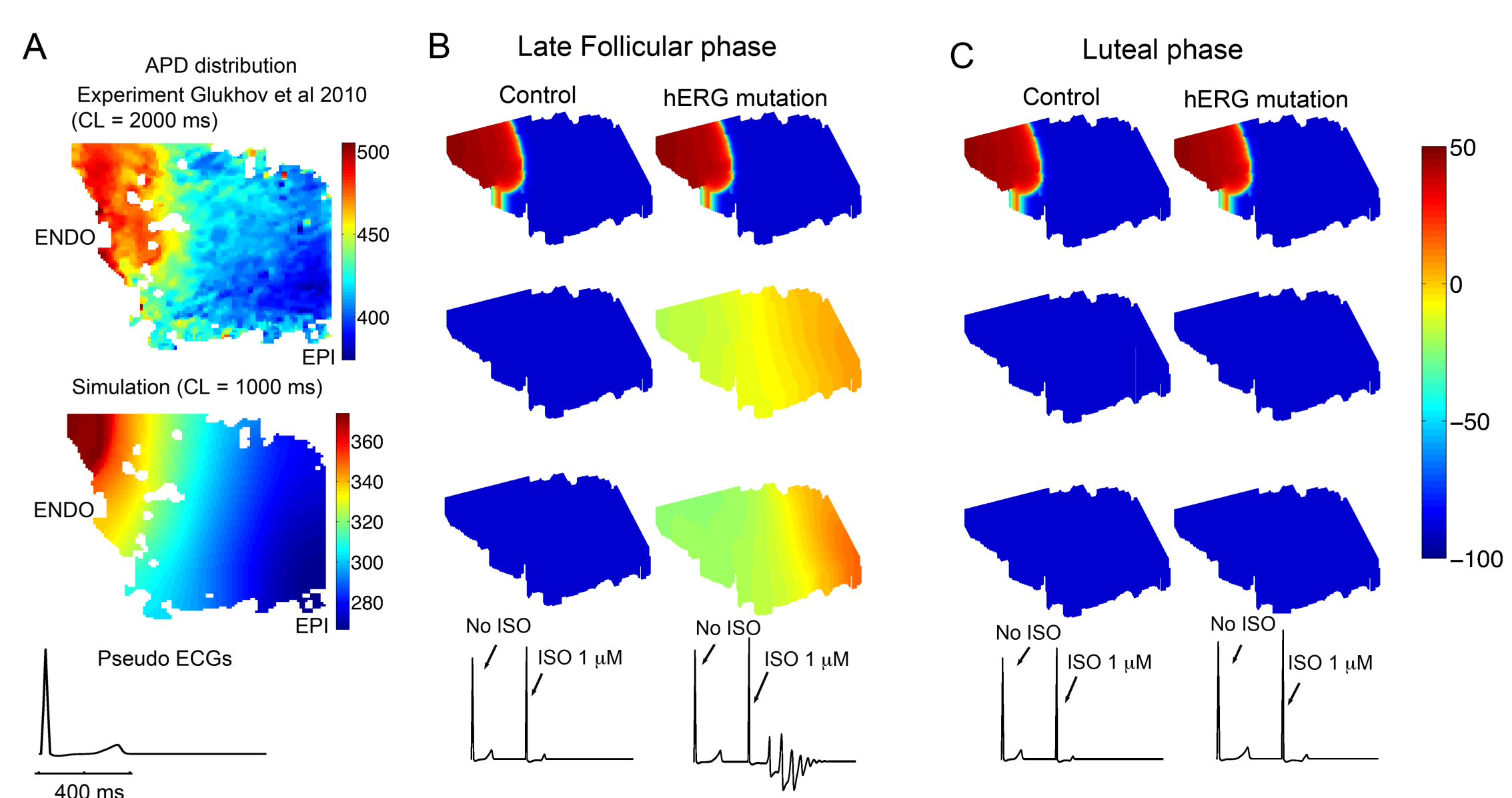


Single cell action potentials are shown on the top of each panel. Transmural 1D tissue models are shown in the middle. Time is shown on the x-axis and voltage on the z-axis. The pseudo ECG is shown beneath the tissue simulation in each panel.

Simulations in female cells predict that in the presence of the G604S pore mutation, vulnerability to the emergence of arrhythmogenic rhythms upon SNS stimulation is exaggerated in the late follicular phase (panel B) where estrogen is highest.

The prolonged T-wave in females corresponds to longer action potential duration (APD), as observed in the space-time plot, and likely contributes to the arrhythmogenic rhythm that emerges in the late follicular phase (panel B).

6. In silico 3D reconstructed human LQTS type 2 female left ventricular (LV) wedge paced with SNS stimulation applied



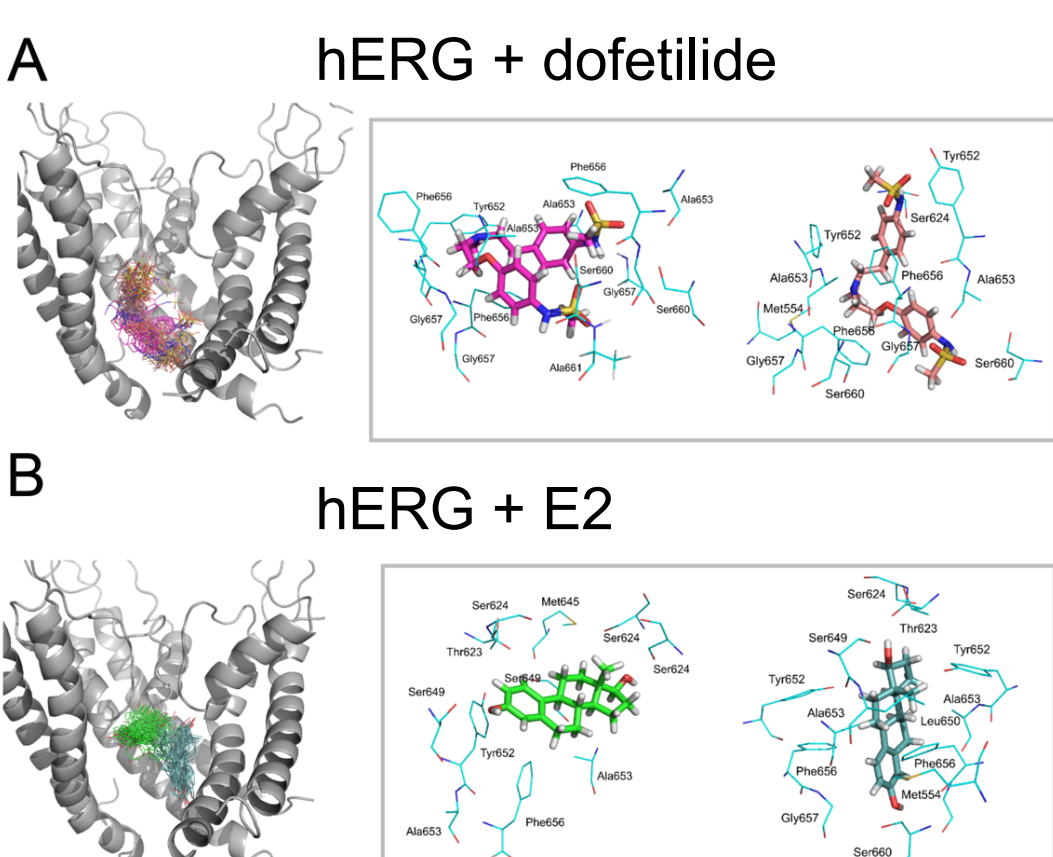
(A) In silico reconstructed human tissue from normal female explanted heart at a pacing rate of 1 Hz. Experimental data from normal human left ventricle from Glukhov et al [8] are shown on the top. Simulated tissue and pseudo ECG are shown in the bottom panel. Action potential duration (APD) variability is indicated by the color scale from long APD80 (red) to short (blue).

(B&C) In the 3D wedge reconstruction with hERG G604S mutation introduced, we observed arousal induced spontaneous arrhythmias in the early follicular (not shown) and late follicular (panel B) phases of menstrual cycle by acute SNS stimulation application. Just as in lower dimensions, the luteal phase (panel C) as well as models without hERG mutation (control) are not predicted to be sensitive to SNS stimulations. Simulated pseudo ECG are shown in the bottom panels.

References

- Yang, PC, Perissinotti, LL, López-Redondo, F, Wang, Y, DeMarco, KR, Jeng, MT, Vorobyov, I, Harvey, RD, Kurokawa, J, Noskov, SY, Clancy, CE. *J Physiol*. 2017. 595(14):4695-723.
- Romero L, Trenor B, Yang P, Saiz J, Clancy CE. *J Mol Cell Cardiol*. 2014. 72:126-37.
- Huo J, Zhang Y, Huang N, Liu P, Huang C, Guo X, Jiang W, Zhou N, Grace A, Huang CL, Ma A, Pflügers Arch. 2008. 456(5):917-28.
- O'Hara T, Virag L, Varro A, Rudy Y. *PLoS Comput Biol*. 2011. 7(5):e1002061.
- Gabriel N, Varro A, La Bouter S, Szuts V, Escande D, Nattel S, Domolombe S. *J Mol Cell Cardiol*. 2010. 49(4):639-46.
- Yang P, Kurokawa J, Furukawa T, Clancy CE. *PLoS Comput Biol*. 2010. 6(1):e1000658.
- O'Hara, T. and Y. Rudy, *Heart Rhythm*. 2012. 9(2):275-82.
- Glukhov AV, Fedorov VV, Lou Q, Ravikumar VK, Kalish PW, Schuessler RB, Moazami N, Efimov IR. *Circ Res* 2010;106:981-991.
- Kurokawa J, Tamagawa M, Harada N, Honda S, Bai CX, Nakaya H, Furukawa T. *J Physiol* 2008 586(12):2961-73.
- Durdagi S, Deshpande S, Duff HJ, Noskov SY. *J Chem Inf Model* 2012 52(10):2760-74.
- Wang YB, Guo JQ, Perissinotti LL, Lees-Miller J, Teng GQ, Durdagi S, Duff HJ, Noskov SY. *Sci Rep* 2016 6: 32536.
- Robertson JL, Palmer LG, Roux B. *J Gen Physiol* 2008 132(6):613-32.

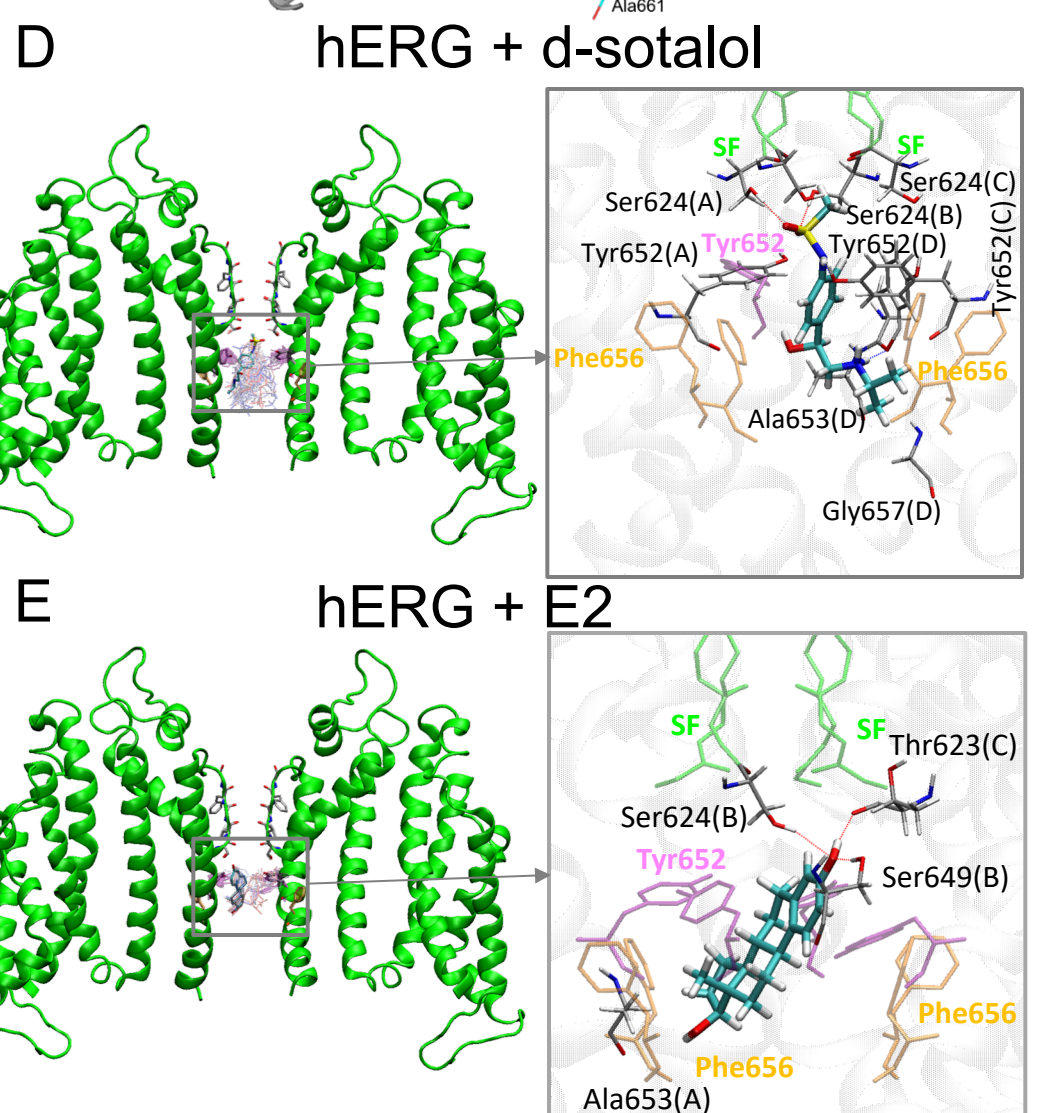
7. Atomistic modeling of a structural basis of acquired LQTS: estradiol (E2) and/or drug binding to hERG intracellular cavity



Top scoring docking poses for dofetilide (A,C) and E2 (B,C) in the intracellular cavity (IC) site of hERG (open-state homology model from [10]).

Left panels: Pore domain of the hERG open state model and selected frames showing dofetilide (pink) and E2 (green) binding to the IC. Right panels: Average position of dofetilide (A), and E2 (B) along with coordinating residues within 3.5 Å for two mapped binding sites. Two dominant binding orientations are shown in magenta and pink for dofetilide and in green and light-blue for E2.

Similar low-energy binding poses for dofetilide (A) and E2 (B) in the IC hERG binding site, associated with channel blockade and acquired LQTS. Dofetilide binding is more favorable by 1.2 kcal/mol (10%) in the presence of E2 in IC (C), suggesting enhancement of blockade and exacerbation of LQTS associated arrhythmias.

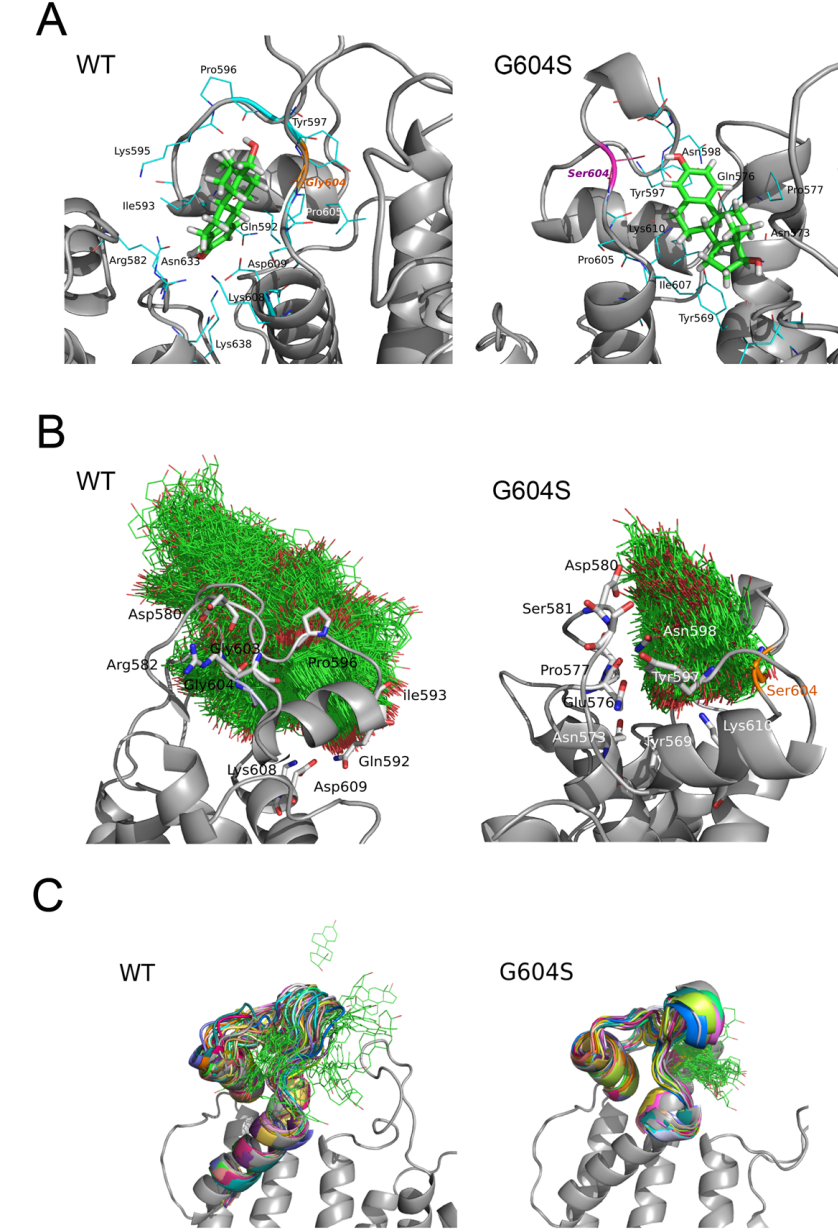


Top scoring docking poses for d-sotalol (D) and E2 (E) in the IC site of hERG (cryo-EM structure PDB ID 5VA1 was used).

Left panels: hERG chains A & C and top 50 dofetilide (D) or E2 (E) binding poses shown as red (lower score) to blue (higher score) sticks. Y652 – pink sticks, F656 – orange sticks. Right panels: The lowest score dofetilide (D) or E2 (E) binding poses shown as thick sticks (cyan-C, O-red, N-blue, S-yellow, H-white) with hERG residues within 3.5 Å shown as thin element-colored sticks (C-gray, other elements as above).

Similar low-energy binding poses for d-sotalol (D) and E2 (E) in the IC hERG binding site, using new channel structure and different methodology.

8. Atomistic modeling of a structural basis of inherited LQTS type 2 sex dependence: E2 binding to pore loop G604S mutant.



Estradiol (E2) binding to a pore loop site of hERG from molecular docking (A), and molecular dynamics (B&C) simulations for WT (left) and G604S mutant channel (right). (homology models based on Eag1, PDB ID 5K7L).

(A) Top scoring docking poses for E2 in the pore-loop site shown together with coordinating residues within 3.5 Å for mapped binding sites.

(B) E2 positions (green wireframe) are mapped from the frames collected in 40 ns MD for WT and G604S mutant to illustrate the conformational space explored by the ligand in the two systems. E2 is kinetically stabilized (trapped) in the G604S mutant, while it is unable to bind stably in the WT.

(C) A G604S mutation is predicted to enhance stability of the bound E2 (green wireframe) in the binding pocket by controlling binding site flexibility as shown in different colors for 32 frames from the first 15 ns MD. The mutation stabilizes the binding site allowing for E2 to remain in the pocket. In contrast, E2 readily leaves binding pocket in the WT hERG.

9. CONCLUSIONS

The multiscale modeling and simulation approach have allowed us to predict „the perfect storm“ of hormone concentration, hERG current derangement, and sympathetic stimulation that may explain one mechanism of increased proclivity to inherited and acquired Long-QT dependent arrhythmias in females.

At the molecular level we revealed potential interactions of estrogen with the arrhythmogenic pore-loop hERG mutation (G604S) as well as hERG pore blockers with high proclivity for Long-QT associated arrhythmias.

This study represents a first step toward predicting mechanisms of sex-based arrhythmias that may lead to important developments in risk stratification and may inform future drug design and screening. It also suggests specific therapeutic anti-arrhythmic strategies for women with Long-QT syndrome, which may include specific hormone replacement therapy.

Acknowledgements

The support was provided by by National Institutes of Health NHLBI U01HL126273-02, R01HL128537-01A1, R01HL128170-02 grants; NIGMS R01GM101928-01 grant; American Heart Association, Western States Affiliate GIA (13GRNT14370019), pre-doctoral fellowship (16PRE27260295, to KR); Canadian Institutes for Health Research (MOP-186232) and Heart and Stroke Foundation, Alberta (GIA) (to SYN); PHM Research Partnership fund (UC Davis, Department of Physiology and Membrane Biology) (to CEC and IV), and the National Biomedical Computation Resource through P41GM103426.